Phylogeny and evolution of *Lasiopodomys* in subfamily Arvivolinae based on mitochondrial genomics

Luye Shi[1], Likuan Liu[2], Xiujuan Li[1], Yue Wu[1], Xiangyu Tian[1], Yuhua Shi[1] and Zhenlong Wang[1]

[1] School of Life Sciences, Zhengzhou University, Zhengzhou, Henan, China
[2] School of Life Sciences, Qinghai Normal University, Xining, Qinghai, China

ABSTRACT

The species of *Lasiopodomys* Lataste 1887 with their related genera remains undetermined owing to inconsistent morphological characteristics and molecular phylogeny. To investigate the phylogenetic relationship and speciation among species of the genus *Lasiopodomys*, we sequenced and annotated the whole mitochondrial genomes of three individual species, namely *Lasiopodomys brandtii* Radde 1861, *L. mandarinus* Milne-Edwards 1871, and *Neodon* (*Lasiopodomys*) *fuscus* Büchner 1889. The nucleotide sequences of the circular mitogenomes were identical for each individual species of *L. brandtii*, *L. mandarinus*, and *N. fuscus*. Each species contained 13 protein-coding genes (PCGs), 22 transfer RNAs, and 2 ribosomal RNAs, with mitochondrial genome lengths of 16,557 bp, 16,562 bp, and 16,324 bp, respectively. The mitogenomes and PCGs showed positive AT skew and negative GC skew. Mitogenomic phylogenetic analyses suggested that *L. brandtii*, *L. mandarinus*, and *L. gregalis* Pallas 1779 belong to the genus *Lasiopodomys*, whereas *N. fuscus* belongs to the genus *Neodon* grouped with *N. irene*. *Lasiopodomys* showed the closest relationship with *Microtus fortis* Büchner 1889 and *M. kikuchii* Kuroda 1920, which are considered as the paraphyletic species of genera Microtus. T_{MRCA} and niche model analysis revealed that *Lasiopodomys* may have first appeared during the early Pleistocene epoch. Further, *L. gregalis* separated from others over 1.53 million years ago (Ma) and then diverged into *L. brandtii* and *L. mandarinus* 0.76 Ma. The relative contribution of climatic fluctuations to speciation and selection in this group requires further research.

Subjects Biodiversity, Ecology, Genomics, Molecular Biology, Zoology
Keywords Lasiopodomys, Mitochondrial genomes, Phylogenetic analysis, Arvivolinae

Submitted 30 September 2020
Accepted 6 January 2021
Published 16 March 2021

Corresponding authors
Xiangyu Tian,
201531200038@mail.bnu.edu.cn
Yuhua Shi,
201631200032@mail.bnu.edu.cn

Academic editor
Tony Robillard

Additional Information and Declarations can be found on page 17

DOI **10.7717/peerj.10850**

INTRODUCTION

Although taxonomical and molecular systematics have led to some progress in the relationship between the genus *Lasiopodomys* and its related genera, numerous uncertainties remain unelucidated. The species belonging to this genus was first described by Lataste in 1887 as part of the Arvivolinae Gray 1821 (Cricetidae Fischer 1817) subfamily, which includes the genera *Phaiomys* Blyth 1863, *Microtus* Schrank 1798, and *Neodon* Horsfield 1841 (*Allen, 1940*; *Corbet, 1978*; *Gromov & Polyakov, 1978*; *Liu et al., 2013*; *Wang, 2003*).

The genus *Lasiopodomys* includes three species from different colonial habitats of life—subterranean (*L. mandarinus* Milne-Edwards 1871), aboveground (*L. brandtii* Radde 1861), and plateau (*L. fuscus* Büchner 1889) by *Wilson & Reeder (2005)*—with relatively short tail and densely furred plantar surfaces. However, their generic taxonomy is not universally accepted, specifically in relation to *Phaiomys*, *Microtus*, and *Neodon*. Molecular data have revealed that the narrow-headed vole *Microtus gregalis* Pallas 1779 (formerly included in subgenus *Stenocranius* Katschenko 1901) is closely related to the species belonging to the genus *Lasiopodomys* (*Abramson & Lissovsky, 2012*). Morphological characteristics, such as karyotype (*Gladkikh et al., 2016*) and mating behavior (*Zorenko & Atanasov, 2017*), supported its current taxonomic status as *L. gregalis*. On the other hand, *L. fuscus* is nested in the genus *Neodon* Hodgson 1849 clade based on the longer length of ear and tail and greater number of inner angles in M_1 and M^3 compared with the genus *Lasiopodomys* (*Liu et al., 2012a*); moreover, *CLOCK*, *BMA1*, and *Cytb* gene sequences and their complete mitochondrial genomes supported this taxonomical status (*Abramson et al., 2009a*; *Bannikova et al., 2010*; *Li, Lu & Wang, 2016a*; *Li et al., 2019*; *Liu et al., 2017*). Recent studies have typically recognized *Lasiopodomys* as a separate genus that includes the species *L. mandarinus* and *L. brandtii*; *L. gregalis* was not widely accepted, whereas *L. fuscus* has been transferred to the genus *Neodon* and named *Neodon fuscus*.

According to fossils and molecular data, the genus *Lasiopodomys* originated and speciated during the Pleistocene epoch (~2.58–0.012 million years ago (Ma)) when quaternary glaciations occurred in this period. Nuclear and mitochondrial phylogenetic estimates have shown that *Lasiopodomys* originated ~2.4 Ma, whereas the division between *L. gregalis* and *Lasiopodomys* has been estimated to have occurred 1.8 Ma and that between *L. mandarinus* and *L. brandtii* was estimated at 0.5–0.95 Ma (*Abramson et al., 2009b*; *Petrova et al., 2015*; *Li et al., 2017*). However, chromosome analysis has shown that karyotype evolution has occurred between *L. mandarinus* and *L. brandtii* at ~2.4 Ma, between *Lasiopodomys* and *L. gregalis* at 2.4 Ma, and between other *Microtus* species at 3 Ma (*Gladkikh et al., 2016*).

The species in the genus *Lasiopodomys* inhabit subterranean and aboveground environments and have recently become model species for comparative hypoxia adaptation (*Dong et al., 2018*; *Sun et al., 2018*). Species' adaptation to low oxygen has been reported in numerous studies (*Childress & Seibel, 1998*; *Dong et al., 2018*; *Nevo, 2013*; *Witt & Huerta-Sánchez, 2019*), and most research has focused on animal models in an artificial environment or has compared them with subterranean rats to reveal the mechanisms of hypoxia (*Ashur-Fabian et al., 2004*; *Malik et al., 2012*; *Malik et al., 2016*). The differences in the environmental adaptability of proximal species are closely related to the historical events experienced during evolution, which play a key role in our understanding of the causes of current differences in life history among these species. However, the historical event that caused the *Lasiopodomys* species to adapt to a different environment has rarely been mentioned (*Dong et al., 2018*; *Dong, Wang & Jiang, 2020*).

Mitochondrial DNA are widely used to study the molecular ecology of animals because it is convenient and economical (*Ballard & Rand, 2005*; *de Freitas et al., 2018*; *Kenechukwu, Li & An, 2018*; *Zhang et al., 2018*). However, several studies have reported the limitations of mitochondrial DNA use (*Galtier et al., 2009*), such as recurrent horizontal transfer

(*Bergthorsson et al., 2003*) and adaptive evolution (*Bazin, Glémin & Galtier, 2006*). The mitochondrial genome is involved in respiratory functions, which are closely associated with oxygen availability (*Jain et al., 2016*; *Santore et al., 2002*; *Solaini et al., 2010*).

In the present study, we sequenced the whole mitochondrial genomes of *L. mandarinus*, *L. brandtii*, and *N. fuscus*, which are species with three repeat individuals, using high-throughput sequencing technology and used the complete mitochondrial genomes of related species from the National Center for Biotechnology Information database to clarify the generic taxonomy of *Lasiopodomys* and evolutionary history of adaptation on aboveground and subsurface life. The findings of this research provide evolutionary information regarding the hypoxia adaptation of *Lasiopodomys*.

MATERIALS AND METHODS

Material preparation and DNA sequencing

Total genomic DNA were extracted from the specimens of *L. mandarinus* (collected from 34°52′N, 113°85′E; Specimen No. LM023), *L. brandtii* (collected from 40°53′N, 116°38′E; Specimen No. LB003), and *N. fuscus* (collected from 34°9′N, 100°2′E; Specimen No. LF010) using the TIANamp Genomic DNA Extraction Kit (TIANGEN, DP304). All specimens were stored at the Animal Museum of Zhengzhou University. The Illumina NovaSeq 6000 (Illumina, San Diego, CA, USA) platform was used for sequencing the samples with a short-insert of 150 bp at ORI-GENE Company, Beijing (https://www.origene.com/).

Genome assembly and annotation

NOVOPlasty 3.6 was used for *de novo* assembly using the mitochondrial genome of *L. mandarinus* (GenBank no. JX014233) as a reference (*Dierckxsens, Mardulyn & Smits, 2017*). All mitochondrial genomes were annotated using GeSeq (*Tillich et al., 2017*), OGDRAW (*Lohse et al., 2013*), and GB2sequin (*Lehwark & Greiner, 2019*) in the MPI-MP CHLOROBOX integrated web tool (https://www.mpimp-golm.mpg.de/chlorobox), which contains the function of the HMMER package for protein-coding genes (PCGs) and ribosomal RNA (rRNA) (*Finn, Clements & Edd, 2011*), and tRNAscan-SE v2.0.3 for transfer RNAs (tRNAs) (*Lowe & Eddy, 1997*). Adenine–thymine (AT) skew was calculated as AT skew = (A − T) / (A + T), whereas guanine–cytosine (GC) skew was calculated as GC skew = (G − C)/(G + C). Circular maps were drawn using the CGView Server V 1.0 web tool (http://stothard.afns.ualberta.ca/cgview_server/) for *L. mandarinus*, *L. brandtii*, *L. gregalis* (GenBank no. MN199169), and *N. fuscus* (*Grant & Stothard, 2008*).

Molecular phylogenetic analysis and divergence time estimation

Phylogenetic analyses were performed on the whole mitochondrial genome sequences (Appendix S1). Besides the nine mitochondrial genomes that were acquired for the present study, five previously published mitochondrial genomes from *L. mandarinus*, *L. gregalis*, and *N. fuscus* were included; therefore, overall, 37 complete mitochondrial genome sequences from 23 species from the subfamily Arvivolinae were considered for phylogenetic analysis. Moreover, three species from *Cricetulus* Milne-Edwards 1867 were chosen as the outgroup. All these sequences were aligned using MAFFT v7.450 (*Katoh &*

Standley, 2013). The nucleotide diversity of the PCGs of *Lasiopodomys* and Arvivolinae was determined using the DNASP v6.12.03 software (*Rozas et al., 2017*), and the best nucleotide substitution models were constructed using jMODELTEST 2.1.7 and selected using the Akaike information criterion (*Darriba et al., 2012*).

The phylogenetic relationships of the two different matrices as well as the whole mitochondrial genomes and PCG sequence matrices were constructed using the maximum likelihood (ML) approach in IQ-TREE v1.6.12 (*Nguyen et al., 2015*) and Bayesian analysis (BI) in the BEAST v1.8.4 program (*Drummond & Rambaut, 2007*). We conducted analysis using 5000 ultrafast bootstrap replicates and the best-fit model in the IQ-TREE software. To determine the maximum clade credibility trees of two different matrices, BEAST analyses were performed using the GTR+G+I substitution models identified above and the uncorrelated relaxed clocks for clock type (*Drummond et al., 2006*), Yule process for tree prior (*Gernhard, 2008*), and other default parameters. Each Markov chain Monte Carlo of 20,000,000 generations was sampled in every 10,000 generations. The effective sample sizes were estimated using Tracer v1.7 for all parameters more than 200 (*Rambaut et al., 2018*). Maximum clade credibility trees were constructed using TreeAnnotator v1.8.4 with a burn-in of the first 20% of the sampled trees (*Drummond & Rambaut, 2007*). Positive selection in all 13 PCGs was determined using branch models and branch-site models via phylogenetic analysis using ML (PAML4.7) programs (*Yang, 2007*). Branch models were used with the one-ratio model, i.e., all the species had the same ω ratio, and the $\omega = 1$ model, with all species in natural selection. Based on the phylogenetic tree, we estimated the ω values of each PCG. The branch-site models used all *Lasiopodomys* species as the foreground branches, and the likelihood ratio test (LRT) was conducted to assess the statistical significance of positive selection.

The molecular divergence time was estimated using the Yule and birth–death processes for trees before implementing phylogeny construction using BEAST v1.8.4 (*Gernhard, 2008*; *Heath, Huelsenbeck & Stadler, 2014*). Marginal likelihood estimation for path sampling and stepping-stone sampling (*Xie et al., 2011*) using 5,000,000 in chain lengths of 500 path steps was used to sample the likelihood of every 5,000 chains (*Baele et al., 2012*; *Baele et al., 2013*). We applied three constraints to calibrate the tree at three prior nodes: (1) the divergence time of the Taiwan vole, *Microtus kikuchii* Kuroda 1920, and the reed vole *Microtus fortis*, of which the split between the subgenus *Alexandromys* Ognev 1914 and *Pallasiimus* Schrank 1798 was estimated via molecular clock analysis at $\sim$1.19 $\pm$ 0.19 Ma (*Bannikova et al., 2010*; *Gao et al., 2017*), (2) the earliest known fossil of *Eothenomys* Allen 1924 at 2.0 Ma (*Liu et al., 2012a*; *Kohli et al., 2014*), and (3) the oldest fossil of Arvicola, which was estimated at 3.0–3.5 Ma (*Abramson et al., 2009a*; *Chen et al., 2012*); we used the mean value of 3.25 Ma.

Ecological niche modeling

The maximum entropy (Maxent) method was used to predict the current potential geographic distributions of *L. mandarinus*, *L. brandtii*, *L. gregalis*, and *N. fuscus* as well as their suitable distributions during the mid-Holocene, 6,000 years ago (kya), Last Glacial Maximum (LGM; 22 kya), and Last Interglacial (LIG; 120–140 kya) epochs (*Phillips,*

Anderson & Schapire, 2006; *Elith et al., 2011*). Presence records were obtained for all four species according to the GBIF database and published papers (Appendix S2). Climatic variables with 19 bioclimatic layers were obtained from the database WorldClim version 1.4 at a resolution of 2.5 arc-minute grid format (*Hijmans et al., 2005*). The potential distributions of the species during the LGM and Holocene periods were predicted using both MIROC-ESM and CCSM4 models (*Watanabe et al., 2011*; *Shields et al., 2012*). Strongly correlated bioclimatic layers ($r > 0.9$) as determined using Pearson's correlation analysis in R 3.6.2 (Appendix S3) (*R Development Core Team, 2013*) were excluded. Moreover, Maxent was independently performed among these species using area under the receiver operating characteristic curve (AUC) prediction model evaluation (*DeLong, DeLong & Clarke-Pearson, 1988*; *Fawcett, 2006*).

RESULTS

The whole mitochondrial genome length of *L. mandarinus* was 16,562 bp, with the same sequences among repeated individuals. The mitochondrial genome length of *L. brandtii* was only 5 bp shorter than that of *L. mandarinus*, whereas that of *N. fuscus* was 220 bp shorter than that of *L. mandarinus* (Fig. 1). On the other hand, *L. mandarinus* was found to be 234 bp longer than the former sequenced mitogenomes (GenBank no. KF819832 & JX014233). All sequences of the three species were longer than those of *L. gregalis*, a species previously in the genus *Microtus*, with sequence lengths of 16,292 bp (GenBank no. MN199169) and 16,294 bp (GenBank no. MN199170). All the three mitogenomes were assembled into a typical circular map with 13 PCGs, 22 tRNAs, 2 rRNAs (rrn12 and rrn16), and a D-loop region (Fig. 1, Table 1). Five types of start codons—ATA, ATC, ATG, ATT, and GTG—were identified among the PCGs, whereas three types of stop codons were identified for these species.

The nucleotide composition of *L. brandtii*, *L. mandarinus*, and *N. fuscus* was biased for A+T by 59.5%, 59.5%, and 58.4%, respectively. All these mitogenomes showed a positive AT skew of 0.08 for *L. brandtii*, 0.09 for *L. mandarinus*, and 0.09 for *N. fuscus*. However, these species showed a negative GC skew ranging from −0.30 for *L. brandtii* to −0.34 for *L. mandarinus* (Fig. 1, Table 2). *L. gregalis* showed higher AT skew (0.10) and GC skew (−0.30) compared with the other three species. Among the 13 PCGs in these 4 species, nucleotide composition ranged from −0.69 in *ATP8* to −0.16 in *ND4L* for *L. mandarinus*, with a GC skew ranging from −0.14 in *ND4L* for *L. brandtii* to 0.33 in *ND6* for *L. mandarinus*. Similarly, all 13 PCGs exhibited a negative GC skew; however, *COX1*, *ND4L* in all species, *COX3* in *L. brandtii* and *L. mandarinus*, and *ND3* in *N. fuscus* showed a negative AT skew and *ND3* in *L. brandtii* and *L. mandarinus* had an AT skew of 0 (Table 2).

The nucleotide diversity among the published Arvicolinae mitogenome sequences and our study species was 0.1429 ± 0.0001, whereas the nucleotide diversity of the mitogenomes of *Lasiopodomys* was 0.0836 ± 0.0155 (Fig. 2). The total nucleotide diversity in all 13 PCGs of Arvicolinae and the genus *Lasiopodomys* was 0.1603 ± 0.0027 and 0.0953 ± 0.0180, respectively (Fig. 2). In Arvicolinae, nucleotide diversity ranged from 0.1378 ± 0.0049 in *Cytb* to 0.1977 ± 0.0077 in *ND3*, whereas for *Lasiopodomys*, it ranged from 0.0829 ± 0.0157 in *COX3* to 0.1256 ± 0.021 in *ND4L*.

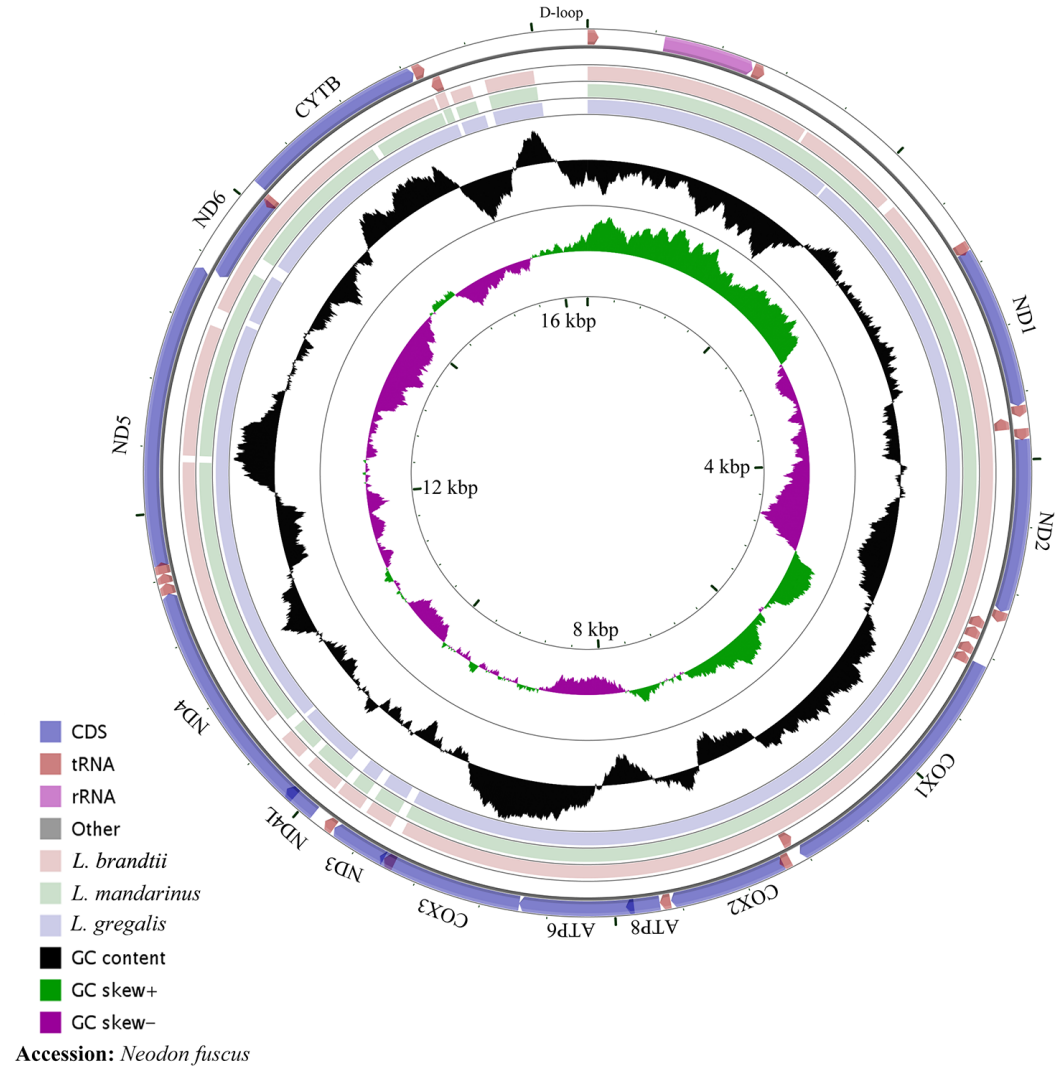

Figure 1 **The complete mitochondrial genome map and GC skew of *Neodon fuscus*, *Lasiopodomys brandtii*, *L. mandarinus*, and *L. gregalis*.**

Full-size DOI: 10.7717/peerj.10850/fig-1

The results of the ML and Bayesian approaches were applied to the datasets of the whole mitogenomes, and the 13 PCG matrices inferred the same topology of the phylogenetic tree structure (Fig. 3). Our results supported that *Lasiopodomys*, *Microtus*, and *Neodon* have close relationships with the basal group of *Proedromys* Thomas 1911. Furthermore, the phylogenetic tree suggested that *L. brandtii*, *L. mandarinus*, and *L. gregalis* formed the genus of *Lasiopodomys*, whereas *N. fuscus* showed a close relationship with *N. irene*, belonging to the genus *Neodon*. *Microtus* was subdivided into two groups: one containing *M. fortis* and *M. kikuchii*, which were strongly supported as the sister group to *Lasiopodomys*, and the other was the basal group of the above species.

In the branch models, the one-ratio model was determined as superior to the $\omega = 1$ model ($df = 1, p < 0.01$), suggesting that all the PCGs in the mitogenomes of *Lasiopodomys*

Table 1 Characteristics of the mitochondrial genome of Neodon fuscus, *Lasiopodomys brandtii, L. mandarinus*, and *L. gregalis*.

Genes	Position (bp)				Strat/stop codon			
	L. brabdtii	*L. mandarinus*	*L. gregalis*	*Neodon fuscus*	*L. brabdtii*	*L. mandarinus*	*L. gregalis*	*Neodon fuscus*
trnF-GAA	1-66	1-66	1-66	1-66				
rrn12	69–1017	69–1018	69–1017	69–1015				
trnV-UAC	1019–1087	1019–1088	1018–1087	1016–1086				
rrn16	1088–2641	1089–2652	1088–2649	1087–2648				
trnL-UAA	2650–2724	2655–2729	2651–2725	2650–2724				
ND1	2710–3681	2715–3686	2726–3680	2725–3679	GTG/TAG	GTG/TAG	GTG/TAG	GTG/TAG
trnI-GAU	3680–3748	3685–3752	3681–3748	3680–3747				
trnQ-UUG	3746–3817	3750–3821	3746–3817	3745–3816				
trnM-CAU	3820–3888	3823–3891	3820–3888	3818–3886				
ND2	3889–4923	3865–4926	3889–4923	3887–4921	ATC/TAA	ATC/TAA	ATT/TAA	ATC/TAA
trnW-UCA	4925–4991	4928–4994	4925–4991	4923–4989				
trnA-UGC	4993–5061	4996–5064	4993–5061	4991–5059				
trnN-GUU	5064–5133	5067–5136	5064–5133	5062–5131				
trnC-GCA	5168–5235	5171–5237	5167–5234	5163–5230				
trnY-GUA	5236–5302	5238–5303	5235–5301	5231–5297				
COX1	5268–6848	5296–6849	5303–6847	5299–6843	ATG/TAA	ATG/TAA	ATG/TAA	ATG/TAA
trnS-UGA	6846–6914	6847–6915	6845–6913	6841–6909				
trnD-GUC	6918–6985	6919–6986	6918–6985	6913–6980				
COX2	6978–7670	6979–7671	6987–7670	6982–7665	ATG/TAA	ATG/TAA	ATA/TAG	ATG/TAA
trnK-UUU	7674–7737	7675–7738	7674–7738	7669–7732				
ATP8	7738–7941	7739–7942	7739–7942	7733–7936	ATG/TAA	ATG/TAA	ATG/TAA	ATG/TAA
ATP6	7899–8579	7900–8580	7900–8580	7894–8574	ATG/TAA	ATG/TAA	ATG/TAA	ATG/TAA
COX3	8474–9412	8508–9413	8580–9363	8574–9357	ATG/TAG	ATG/TAG	ATG/TAG	ATG/TAG
trnG-UCC	9363–9430	9364–9431	9364–9431	9358–9426				
ND3	9431–9778	9432–9779	9432–9779	9427–9774	ATT/TAA	ATT/TAA	ATT/TAA	GTG/TAA
trnR-UCG	9780–9846	9781–9847	9781–9847	9776–9842				
ND4L	9849–10145	9851–10147	9850–10146	9844–10140	ATG/TAA	ATG/TAA	ATG/TAA	ATG/TAA
ND4	9962–11521	10141–11523	10140–11517	10134–11511	ATG/TTA	ATG/TTA	ATG/TTA	ATG/TTA
trnH-GUG	11517–11583	11519–11584	11518–11585	11512–11579				
trnS-UCU	11584–11642	11585–11643	11586–11644	11580–11638				
trnL-UAG	11642–11711	11643–11712	11644–11713	11638–11707				
ND5	11691–13523	11692–13524	11714–13525	11708–13519	ATT/TAA	ATT/TAA	ATA/TAA	ATA/TAA
ND6	13520–14104	13521–14147	13522–14046	13516–14040	ATG/TTA	ATG/TTA	ATG/TTA	ATG/TTA
trnE-UUC	14042–14110	14046–14114	14047–14115	14041–14109				
Cytb	14113–15258	14117–15262	14121–15263	14115–15257	ATG/TAA	ATG/TAA	ATG/TAA	ATG/TAA
trnT-UGU	15260–15326	15265–15331	15265–15331	15260–15327				
trnP-UGG	15566–15633	15522–15589	15332–15399	15328–15395				

undergo purifying selection (Table 3). In the branch-site model, only the ATP6 gene was present in some positive selection sites (60I 0.987, $p < 0.01$) in *Lasiopodomys* (Table 3). Moreover, positive selection sites were predicted in *Cox1*, *Cox3*, *Cytb*, *ND2*, *ND3*, and *ND5*. However, the LRTs were not significant.

Table 2 Nucleotide composition data for the PCGs and whole mitochondrial genomes of *Neodon fuscus, Lasiopodomys brandtii, L. mandarinus*, and *L. gregalis*.

Species	contents	T	C	A	G	GC skew	AT skew
L. brabdtii	*whole*	27.4	26.4	32.1	14.1	−0.30	0.08
	ATP6	28.3	29.8	31	10.9	−0.46	0.05
	ATP8	26	27	37.7	9.3	−0.49	0.18
	COX1	29.5	25.5	27.1	18	−0.17	−0.04
	COX2	26.3	27.7	31.6	14.4	−0.32	0.09
	COX3	29.3	26.8	28.6	15.4	−0.27	−0.01
	cytB	27	29.1	30.5	13.4	−0.37	0.06
	ND1	28.5	28.9	30.7	11.9	−0.42	0.04
	ND2	26.7	31	33.9	8.4	−0.57	0.12
	ND3	30.7	26.1	30.5	12.6	−0.35	0.00
	ND4	27.8	28.3	31	12.9	−0.37	0.05
	ND4L	31.3	30.3	23.6	14.8	−0.34	−0.14
	ND5	28	27.8	32.4	11.8	−0.40	0.07
	ND6	20.6	30.9	38.6	9.9	−0.51	0.30
L. gregalis	*whole*	26.5	27.2	32.1	14.2	−0.31	0.10
	ATP6	17.6	30.5	29.8	12	−0.44	0.26
	ATP8	24.5	29.4	38.7	7.4	−0.60	0.22
	COX1	28.7	26.5	26.9	18	−0.19	−0.03
	COX2	28.3	26.1	30	15.6	−0.25	0.03
	COX3	27.6	28.4	29.1	14.9	−0.31	0.03
	cytB	26.5	29.7	30.3	13.5	−0.38	0.07
	ND1	25.9	31.5	30	12.6	−0.43	0.07
	ND2	26.1	29.7	35	9.3	−0.52	0.15
	ND3	27.3	29.9	30.7	12.1	−0.42	0.06
	ND4	27.1	29.4	31.9	11.4	−0.44	0.08
	ND4L	30.6	31.3	26.6	11.4	−0.47	−0.07
	ND5	25.9	30.4	31.5	12.3	−0.42	0.10
	ND6	22.4	29.4	39.6	8.7	−0.54	0.28
L. mandarinus	*whole*	27.1	27.1	32.4	13.4	−0.34	0.09
	ATP6	29.8	29.2	30.7	10.3	−0.48	0.01
	ATP8	27.9	28.9	37.7	5.4	−0.69	0.15
	COX1	28.7	26.5	27.7	17.1	−0.22	−0.02
	COX2	27	27.1	32.5	13.4	−0.34	0.09
	COX3	29	28.4	28	14.6	−0.32	−0.02
	cytB	26.5	30.7	30.6	12.1	−0.43	0.07
	ND1	28.4	29.1	30.2	12.2	−0.41	0.03
	ND2	26.9	30.9	33.9	8.3	−0.58	0.12
	ND3	32.2	24.1	32.2	11.5	−0.35	0.00
	ND4	28	28.5	32.3	11.2	−0.44	0.07
	ND4L	32	29.3	26.6	21.1	−0.16	−0.09
	ND5	27	28.9	33	11.2	−0.44	0.10
	ND6	20	30.7	40.1	9.2	−0.54	0.33

(*continued on next page*)

Table 2 (*continued*)

Species	contents	T	C	A	G	GC skew	AT skew
Neodon fuscus	*whole*	26.5	27.2	31.9	14.4	−0.31	0.09
	ATP6	27.6	31.3	28.8	12.3	−0.44	0.02
	ATP8	27	27	37.7	8.3	−0.53	0.17
	COX1	29	26.4	26.6	18	−0.19	−0.04
	COX2	26.8	26.8	31.5	14.9	−0.29	0.08
	COX3	27.1	29.5	28	15.4	−0.31	0.02
	cytB	25.8	31.3	28.8	14	−0.38	0.05
	ND1	25.9	30.7	31	12.4	−0.42	0.09
	ND2	25.7	30.7	35	8.6	−0.56	0.15
	ND3	29.6	28.2	28.2	14.1	−0.33	−0.02
	ND4	27	29.1	31	12.9	−0.39	0.07
	ND4L	29.2	30.2	26.8	13.8	−0.37	−0.04
	ND5	26.2	29.8	31.5	12.5	−0.41	0.09
	ND6	21.8	28.8	39.9	9.4	−0.51	0.29

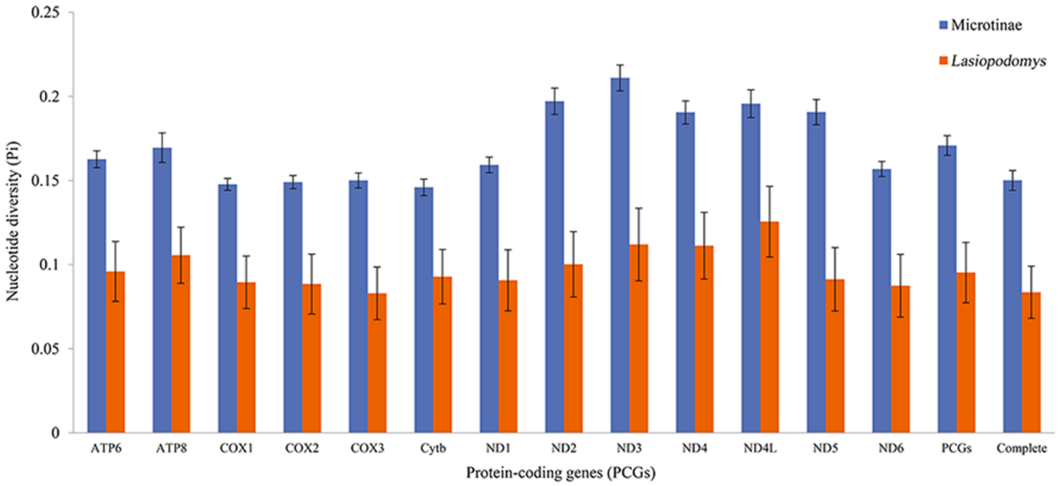

Figure 2 **Nucleotide diversity of each protein-coding gene (PCG), concatenate PCG, and whole mitochondrial genomes of Microtinae (blue) and *Lasiopodomys* (orange).**
Full-size DOI: 10.7717/peerj.10850/fig-2

The species divergence time among the *Lasiopodomys* species and related genera was calculated using the uncorrelated relaxed molecular clock model, which was calibrated with three prior divergence times of Arvicolinae (Fig. 3). The results suggested that the origin of *Lasiopodomys* was no earlier than the early Pleistocene epoch (∼0.781–2.58 Ma), with a possible most common ancestor of *Lasiopodomys* at ∼1.79 Ma (95% HPD values: ∼1.52–2.09 Ma). The split between *L. brandtii* and *L. mandarinus* was dated to the early Pleistocene period at ∼0.76 Ma (95% HPD values: ∼0.58–0.98 Ma), whereas the separation of both from *L. gregalis* was dated to the early Pleistocene epoch at 1.53 Ma (95% HPD values: ∼1.26–1.81 Ma). The estimated divergence event of *N. fuscus* and *N. irene* was found to be during the early Pleistocene epoch at 1.44 Ma (95% HPD Interval: ∼1.12–1.75 Ma).

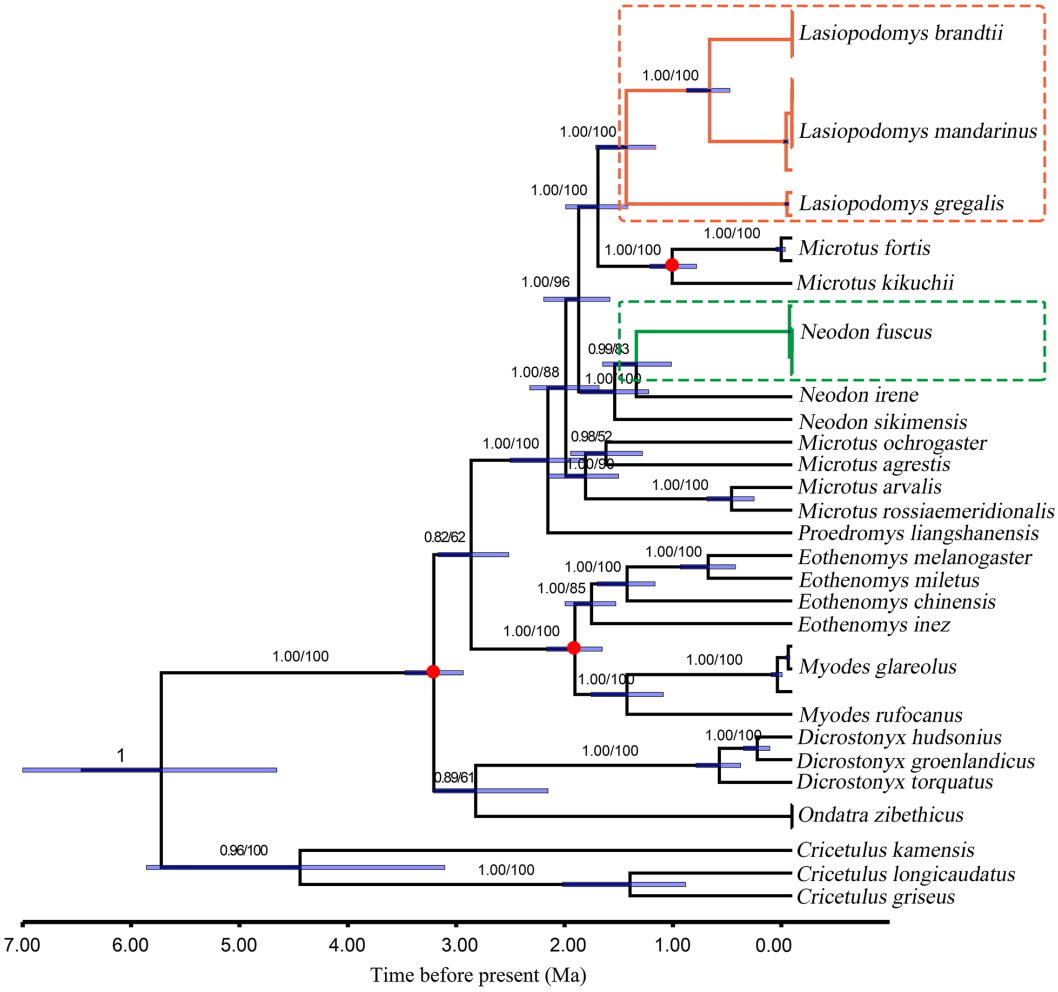

Figure 3 Divergence time for *Lasiopodomys* with whole mitochondrial genomes. The numbers on each node are posterior probabilities and bootstrap values. Blue bars show 95% highest posterior density intervals of node heights. Three red circles were fossil time. The genus of *Cricetulus* was used as an outgroup.
Full-size DOI: 10.7717/peerj.10850/fig-3

The high AUC values determined via ecological niche modeling (ENM) indicated the good performance of the model predictions of this study (Appendix S4). During the periods from the LIG to present, all species of *Lasiopodomys* showed no evident loss of a suitable habitat. A western expansion of *L. brandtii* has been predicted in Northeast China, Inner Mongolia, and South Siberia, whereas a weak fragment was predicted for *L. gregalis* among the Eurasia regions (Fig. 4). Moreover, suitable areas were predicted in highly suitable habitat regions during the LGM in these species. More northern suitable areas were predicted during the LIG, and a northern expansion was predicted during the transition from the Holocene period to the present (Fig. 4). In addition, highly suitable habitats were observed for *N. fuscus* in the Hengduan Mountains during all periods, whereas more eastern distributions were predicted during the LGM (Fig. 4).

Table 3 **Likelihood ratio tests of branch models and branch-site models examining the proteincoding genes of the genus *Lasiopodomys*.**

Gene	Model		lnL	Models compared	Parameter Estimates	LRT (*P*-value)
ATP6	Branch-model	A:One-ratio	−6321.793406		ω= 0.02625	$p < 0.01$
		B:Omega = 1	−7802.578602	B vs A	ω=1	
	Branch-site model	Null	−6298.662308	null vs A	7 A 0.578	P<0.01
		Model A	−6295.340396		60 I 0.987*	
ATP8	Branch-model	A:One-ratio	−2156.664937		ω=0.16120	$p < 0.01$
		B:Omega = 1	−2304.668614	B vs A	ω=1	
	Branch-site model	Null	−2092.811906			1
		Model A	−2092.811906	null vs A	NA	
Cox1	Branch-model	A:One-ratio	−12806.04872	B vs A	ω=0.00534	$p < 0.01$
		B:Omega = 1	−17316.74494		ω=1	
	Branch-site model	Null	−12712.24034	null vs A	57 I 0.779	0.077
		Model A	−12710.67689		487 T 0.965*	
Cox2	Branch-model	A:One-ratio	−5779.531238		ω=0.01386	$p < 0.01$
		B:Omega = 1	−7512.338542	B vs A	ω=1	
	Branch-site model	Null	−5711.411586			1
		Model A	−5711.411586	null vs A	NA	
Cox3	Branch-model	A:One-ratio	−6864.103188		ω=0.01989	$p < 0.01$
		B:Omega = 1	−8741.926003	B vs A	ω=1	
	Branch-site model	Null	−6757.123306			
		Model A	−6757.116417	null vs A	50 N 0.642 62 V 0.517 203 F 0.593	0.9065
Cytb	Branch-model	A:One-ratio	−10097.89327		ω=0.02761	$p < 0.01$
		B:Omega = 1	−12504.74705	B vs A	ω=1	
	Branch-site model	Null	−10010.08824			
		Model A	−10009.07827	null vs A	4 M 0.976* 7 K 0.892 116 I 0.567 242 V 0.522 315 I 0.516	0.1552

(*continued on next page*)

Table 3 (*continued*)

Gene	Model		lnL	Models compared	Parameter Estimates	LRT (*P*-value)
ND1	Branch-model	A:One-ratio	−9200.160474		ω=0.02426	
		B:Omega = 1	−11391.13236	B vs A	ω=1	$p < 0.01$
	Branch-site model	Null	−9015.80101			
		Model A	−9015.745075	null vs A	NA	0.738
ND2	Branch-model	A:One-ratio	−11468.97809		ω=0.06165	
		B:Omega = 1	−13190.51757	B vs A	ω=1	$p < 0.01$
		Null	−11268.21175			
	Branch-site model	Model A	−11268.21175	null vs A	11 F 0.747 14 F 0.816 31 I 0.845 95 T 0.837 122 I 0.856 207 I 0.845 220 H 0.867 228 K 0.847 235 N 0.860 241 L 0.858	1
ND3	Branch-model	A:One-ratio	−4086.367921		ω=0.06686	
		B:Omega = 1	−4686.550566	B vs A	ω=1	$p < 0.01$
		Null	−3969.046821			
	Branch-site model	Model A	−3969.013478	null vs A	6 A 0.811 14 S 0.790 20 V 0.861 108 Q 0.849	0.7962
ND4	Branch-model	A:One-ratio	−15050.32692		ω=0.04173	
		B:Omega = 1	−17886.34941	B vs A	ω=1	$p < 0.01$
	Branch-site model	Null	−14856.89331			
		Model A	−14856.89325	null vs A	NA	0.992

(*continued on next page*)

Table 3 (*continued*)

Gene	Model		lnL	Models compared	Parameter Estimates	LRT (*P*-value)
ND4L	Branch-model	A:One-ratio	−3210.084127		ω=0.05007	
		B:Omega = 1	−3775.223753	B vs A	ω=1	$p < 0.01$
	Branch-site model	Null	−3151.8857			
		Model A	−3151.8857	null vs A	NA	1
ND5	Branch-model	A:One-ratio	−19894.46685		ω=0.04666	
		B:Omega = 1	−23436.47839	B vs A	ω=1	$p < 0.01$
	Branch-site model	Null	−19737.31375			
		Model A	−19737.31225	null vs A	194 E 0.512 575 K 0.969*	0.9563
ND6	Branch-model	A:One-ratio	−5081.893461		ω=0.06927	
		B:Omega = 1	−5814.462234	B vs A	ω=1	$p < 0.01$
	Branch-site model	Null	−4971.821282			
		Model A	−4971.821283	null vs A	NA	1

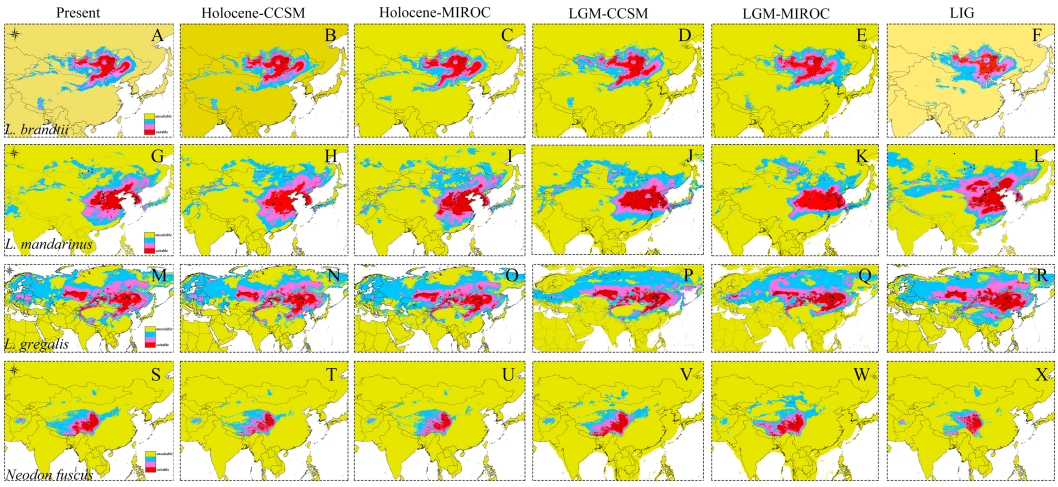

Figure 4 **Ecological niche modeling of *Lasiopodomys* and *Neodon*.** *Lasiopodomys brandtii* (A–F), *L. mandarinus* (G–L), *L. gregalis* (M–R), and *Neodon fuscus* (S–X) under the current climate and three periods in the past: the mid-Holocene, the Last Glacial Maximum (LGM), and the Last Interglacial Maxima (LIG).

Full-size DOI: 10.7717/peerj.10850/fig-4

DISCUSSION

Structural features of the whole mitochondrial genome of *Lasiopodomys*

Among the nine complete mitochondrial sequences, all the species showed same sequences in the three repeated individuals, thereby supporting the accuracy and low intraspecific variation of our studies (*Brown & Simpson, 1981*). Although *N. fuscus* showed similar characteristics to previously sequenced mitogenomes (GenBank no. MG833880), *L. mandarinus* exhibited a longer sequence than that previously reported (*Cong et al., 2016*; *Li, Lu & Wang, 2016a*; *Li et al., 2016b*; *Li et al., 2019*). This difference may be due to nucleotide errors, particularly in tandem repeats, caused by different sequencing technologies: Sanger sequencing versus high-throughput sequencing (*Pfeiffer et al., 2018*). All these differences occurred in the intergenic region, with little impact on subsequent analysis. Therefore, we reserved both types of sequence data in the subsequent analysis.

All the PCGs of these species, similar to the other Arvicolinae mitogenomes, had an incomplete stop codon that was automatically filled during the transcription process in the mitogenomes of animals, with no effect on translation (*Ojala, Montoya & Attardi, 1981*). Similar to previous studies, the nucleotide diversity of all the PCGs in both *Lasiopodomys* and Arvicolinae typically showed the highest divergence in the NADH dehydrogenase complex and the lowest divergence in the cytochrome c oxidase subunit complex and cytochrome B gene (*Huang et al., 2019*; *Ramos et al., 2018*). The nucleotide sequence diversity of the NADH dehydrogenase gene groups may be affected by variations in the historical environment (*Ramos et al., 2018*; *Mueller, 2006*). Similar to previously published mitogenomes, the AT skew of *Lasiopodomys* and *N. fuscus* was consistent with that of vertebrates (*Zhang, Cheng & Ge, 2019*; *Martin, 1995*), further indicating evolutionary

pressure related to the mechanism of DNA replication (*Charneski et al., 2011*; *Dai & Holland, 2019*).

Phylogenetic relationships of *Lasiopodomys*

Our molecular phylogenetic analysis results were highly consistent those of previous studies. In our study, the subfamily Arvicolinae was supported as a monophyletic group based on the molecular data of *Cytb*, *COX1*, *GHR*, *CLOCK*, and *BMAL1* (*Abramson et al., 2009b*; *Buzan et al., 2008*; *Liu et al., 2017*; *Martin et al., 2000*; *Sun et al., 2018*). Our results suggest that *N.* (*Lasiopodomys*) *fuscus* within the genus *Neodon* forms a sister relationship with *N. irene*, consistent with the results reported by *Chen et al. (2012)* and *Li et al. (2019)*. The stable clustering of *L. brandtii*, *L. mandarinus*, and *L. gregalis* into one group confirms the systematic positions of *Lasiopodomys*. This topology was consistent with that of other phylogenetic studies based on nuclear genes (*Sun et al., 2018*), mitochondrial DNA (*Abramson et al., 2009a*; *Liu et al., 2012b*; *Martínková & Moravec, 2012*; *Petrova et al., 2016*), and whole genomes (*Li, Lu & Wang, 2016a*; *Li et al., 2019*; *Tian et al., 2020*). However, it contradicts with the systematic position based on the morphological characteristics of these species (*Allen, 1940*; *Corbet, 1978*; *Wilson & Reeder , 2005*). Further, *L. brandtii* and *L. mandarinus* have consistently presented as a sister group in molecular phylogenetic studies, with seldom distinguished morphological characteristics but different aboveground and underground habitats, suggesting a mechanism of environmental adaptation during rapid speciation (*Alexeeva, Erbajeva & Khenzykhenova, 2015*; *Dong et al., 2018*; *Li et al., 2017*). Other species of *Microtus* and *Neodon* were not found in the monophyletic group (*Liu et al., 2012a*); *M. kikuchii* and *M. fortis* were grouped as sister lineages within the *Lasiopodomys* clades and were considered belonging to the subgenus *Alexandromys* based on phylogenetic research (*Mezhzherin, Zykov & Morozov-Leonov, 1993*), allozymes, and *Cytb* (*Bannikova et al., 2010*). All these genera form a "*Microtus s.* l.," which could be the "core Arvicolinae" (*Baca et al., 2019*).

Evolution and demographic history of *Lasiopodomys*

When inferring the divergence time of *Lasiopodomys* and related genera, both the Yule process and birth–death process speciation models were required with multiple fossil calibration nodes employed in phylogenetic analysis to develop more robust estimates (*Drummond & Rambaut, 2007*; *Humphreys et al., 2016*). Based on complete genomes and PCG phylogenetic trees, both models presented similar estimates of a relatively recent origin and divergence time for *Microtus s.* l. during the early Pleistocene epoch. The oldest reported fossil of *Microtus s.* l. was during the early Pleistocene epoch (*Chaline et al., 1999*). An arid and cold environment raised species dispersal and speciation in response to Pleistocene climatic fluctuations (*Vasconcellos et al., 2019*). Our study supported the first appearance of *Lasiopodomys* in the late early Pleistocene epoch from the Transbaikal area (*Alexeeva, Erbajeva & Khenzykhenova, 2015*; *Li et al., 2017*) at ∼1.52–2.09 Ma (*Petrova et al., 2016*) but later than that estimated by chromosomes at 3 Ma (*Gladkikh et al., 2016*). At ∼1.28–1.81 Ma, the morphological characters of *L. gregalis* proposed the earliest clades of modern *Lasiopodomys*, as indicated by molecular data and fossils (*Abramson et al., 2009a*;

Chaline et al., 1999; *Petrova et al., 2016*). Thereafter, the clades separated into *L. brandtii* and *L. mandarinus* at ~0.58–0.98 Ma in our study, which is similar to inferences from *Cytb* and D-loop sequences (*Li et al., 2017*; *Petrova et al., 2015*) but less similar to the inferences from molecular cytogenetic analyses at ~1.8 Ma (*Gladkikh et al., 2016*).

ENM indicated a considerably wider distribution area of *Lasiopodomys* in the past than in the present, which conforms to the fossils from the Pleistocene period (*Alexeeva, Erbajeva & Khenzykhenova, 2015*). During the early Pleistocene period, continuous cooling formed an arid climate in the high latitudes of the Northern Hemisphere (*Guo et al., 2008*). Climatic changes seldom shifted the suitable habitat of *Lasiopodomys* during the LIG and LGM periods. It is possible to infer that migration events occurred during the extremely cold and dry conditions, with a trend of continuous distribution farther to the northeast during the Pleistocene period until the Holocene period (*Alexeeva, Erbajeva & Khenzykhenova, 2015*; *Prost et al., 2013*). The appearance of *N. fuscus*, which is adapted to plateau climates, was later than the Qinghai-Tibet Plateau uplift (*Wang et al., 2008*), with no significant distributed shifts. All ancient species of *Lasiopodomys* may have been distributed as per their current distribution areas with a radiation evolution (*Abramson et al., 2009b*; *Bannikova et al., 2010*) before the interglacial and glacial periods based on ENM and fossil reports (*Alexeeva, Erbajeva & Khenzykhenova, 2015*; *Petrova et al., 2015*). Considering the lower sensitivity to climatic changes and adaptation to habitat areas, the *Lasiopodomys* species could colonize in north regions; moreover, the evolution of characteristics, such as teeth and densely furred plantar surfaces, further enabled their survival in cooler, drier conditions.

Despite precipitation and temperature fluctuations, a decline in atmospheric O_2also occurred during the past 0.8 Ma (*Stolper et al., 2016*). Environmental stress caused a major driving on evolutionary process (*Parsons, 2005*). In the species of rodents, limited oxygen availability resulted in evolutionary adaptation and appearance of various strategies (*Pamenter et al., 2020*), such as different colonial habitats of life—subterranean (*L. mandarinus*) and plateau (*L. fuscus*); these strategies formed unique physiological and molecular adaptations to hypoxia (*Jiang et al., 2020*; *Dong, Wang & Jiang, 2020*). Our study supports a history of rapid population expansion under positive selection via mitogenome sequences such as the ATP6 gene, which uses oxygen to create adenosine triphosphate. However, further research using integrated phylogeographic analyses of the genus *Lasiopodomys* (*Li et al., 2017*; *Petrova et al., 2015*) is warranted to determine the adaptation of *L. brandtii* and *L. mandarinus* to factors including precipitation, temperature, and chronic hypoxia.

ACKNOWLEDGEMENTS

We would like to thank Yifeng Zhang and Xinrui Wang for their help in feeding the experimental animals.

ADDITIONAL INFORMATION AND DECLARATIONS

Funding

This work was supported by the National Natural Science Foundation of China (grant no. 31372193) and the Key scientific research projects of Henan Higher Education Institutions (grant no. 18A180007). The funders had no role in study design, data collection and analysis, decision to publish, or preparation of the manuscript.

Grant Disclosures

The following grant information was disclosed by the authors:
Natural Science Foundation of China: 31372193.
Key scientific research projects of Henan Higher Education Institutions: 18A180007.

Competing Interests

The authors declare there are no competing interests.

Author Contributions

- Luye Shi conceived and designed the experiments, performed the experiments, prepared figures and/or tables, and approved the final draft.
- Likuan Liu, Xiujuan Li and Yue Wu analyzed the data, prepared figures and/or tables, and approved the final draft.
- Xiangyu Tian conceived and designed the experiments, performed the experiments, prepared figures and/or tables, authored or reviewed drafts of the paper, and approved the final draft.
- Yuhua Shi analyzed the data, authored or reviewed drafts of the paper, and approved the final draft.
- Zhenlong Wang conceived and designed the experiments, authored or reviewed drafts of the paper, and approved the final draft.

Data Availability

The following information was supplied regarding data availability:
Sequences are available at GenBank: MT614214 to MT614219.
Sequences are also available in the Supplementary Files.

Supplemental Information

Supplemental information for this article can be found online at http://dx.doi.org/10.7717/peerj.10850#supplemental-information.

REFERENCES

Abramson NI, Lebedev VS, Bannikova AA, Tesakov AS. 2009a. Radiation events in the subfamily Arvicolinae (Rodentia): evidence from nuclear genes. *Doklady Biological Sciences: Proceedings of the Academy of Sciences of the USSR, Biological Sciences Sections* **428**:458–461 DOI 10.1134/S0012496609050196.

Abramson NI, Lebedev VS, Tesakov AS, Bannikova AA. 2009b. Supraspecies relationships in the subfamily Arvicolinae (Rodentia, Cricetidae): an unexpected result of nuclear gene analysis.. *Molecular Biology* **43**:834–46 DOI 10.1134/S0026893309050148.

Abramson NI, Lissovsky AA. 2012. Subfamily arvicolinae. In: *The mammals of Russia: a taxonomic and geographic reference*. Moscow: Archive of Zoological Museum of MSU. KMK Scientific Press, 220–276.

Alexeeva N, Erbajeva M, Khenzykhenova F. 2015. Lasiopodomys brandti in Pleistocene of Transbaiklia and adjacent territories: distribution area, evolutionary development in context of global and regional events. *Quaternary International* **355**:11–17 DOI 10.1016/j.quaint.2014.08.017.

Allen GM. 1940. *The mammals of China and Mongolia In: Granger W, ed. Natural History of Central Asia*. New York: Central Asiatic Expeditions of the American Museum of Natural History.

Ashur-Fabian O, Avivi A, Trakhtenbrot L, Adamsky K, Cohen M, Kajakaro G, Joel A, Amariglio N, Nevo E, Rechavi G. 2004. Evolution of p53 in hypoxia-stressed Spalax mimics human tumor mutation. *Proceedings of the National Academy of Sciences of the United States of America* **101**:12236–12241 DOI 10.1073/pnas.0404998101.

Baca M, Popović D, Lemanik A, Baca K, Horáček I, Nadachowski A. 2019. Highly divergent lineage of narrow-headed vole from the Late Pleistocene Europe. *Scientific Reports* **9**:17799 DOI 10.1038/s41598-019-53937-1.

Baele G, Lemey P, Bedford T, Rambaut A, Suchard MA, Alekseyenko AV. 2012. Improving the accuracy of demographic and molecular clock model comparison while accommodating phylogenetic uncertainty. *Molecular Biology and Evolution* **29**:2157–2167 DOI 10.1093/molbev/mss084.

Baele G, Li WLS, Drummond AJ, Suchard MA, Lemey P. 2013. Accurate model selection of relaxed molecular clocks in Bayesian phylogenetics. *Molecular Biology and Evolution* **30**:239–243.

Ballard JWO, Rand DM. 2005. The population biology of mitochondrial DNA and its phylogenetic implications. *Annual Review of Ecology, Evolution, and Systematics* **36**:621–642 DOI 10.1146/annurev.ecolsys.36.091704.175513.

Bannikova AA, Lebedev VS, Lissovsky AA, Matrosova V, Abramson NI, Obolenskaya EV, Tesakov AS. 2010. Molecular phylogeny and evolution of the Asian lineage of vole genus *Microtus* (Rodentia: Arvicolinae) inferred from mitochondrial cytochrome b sequence. *Biological Journal of the Linnean Society* **99**:595–613 DOI 10.1111/j.1095-8312.2009.01378.x.

Bazin E, Glémin S, Galtier N. 2006. Population size does not influence mitochondrial genetic diversity in animals. *Science* **312**:570–572 DOI 10.1126/science.1122033.

Bergthorsson U, Adams KL, Thomason B, Palmer JD. 2003. Widespread horizontal transfer of mitochondrial genes in flowering plants. *Nature* **424**:197–201 DOI 10.1038/nature01743.

Brown GG, Simpson MV. 1981. Intra- and interspecific variation of the mitochondrial genome in *Rattus norvegicus* and *Rattus rattus*: restriction enzyme analysis of variant

mitochondrial DNA molecules and their evolutionary relationships. *Genetics* **97**:125–143.

Buzan EV, Krystufek B, Hänfling B, Hutchinson WF. 2008. Mitochondrial phylogeny of Arvicolinae using comprehensive taxonomic sampling yields new insights. *Biological Journal of the Linnean Society* **94**:825–835 DOI 10.1111/j.1095-8312.2008.01024.x.

Chaline J, Brunet-Lecomte P, Montuire S, Viriot L, Courant F. 1999. Anatomy of the arvicoline radiation (Rodentia): palaeogeographical, palaeoecological history and evolutionary data. *Annales Zoologici Fennici* **36**:239–267.

Charneski CA, Honti F, Bryant JM, Hurst LD, Feil EJ. 2011. Atypical AT skew in firmicute genomes results from selection and not from mutation. *PLOS Genetics* **7**:e1002283 DOI 10.1371/journal.pgen.1002283.

Chen W, Hao H, Sun Z, Liu Y, Liu S, Yue B. 2012. Phylogenetic position of the genus *Proedromys* (Arvicolinae, Rodentia): evidence from nuclear and mitochondrial DNA. *Biochemical Systematics and Ecology* **42**:59–68 DOI 10.1016/j.bse.2012.01.002.

Childress JJ, Seibel BA. 1998. Life at stable low oxygen levels: adaptations of animals to oceanic oxygen minimum layers. *The Journal of Experimental Biology* **201**:1223–1232.

Cong H, Kong LM, Liu ZX, Wu Y, Motokawa M, Harada M, Li Y. 2016. Complete mitochondrial genome of the mandarin vole *Lasiopodomys mandarinus* (Rodentia: Cricetidae), Mitochondrial DNA. *Part A, DNA Mapping, Sequencing, and Analysis* **27**:760–761.

Corbet GB. 1978. *The mammals of the Palaearctic region: a taxonomic review*. London: Natural History. British Museum.

Dai Y, Holland PWH. 2019. The interaction of natural selection and GC Skew may drive the fast evolution of a sand rat homeobox gene. *Molecular Biology and Evolution* **36**:1473–1480 DOI 10.1093/molbev/msz080.

Darriba D, Taboada GL, Doallo R, Posada D. 2012. JModelTest 2: more models, new heuristics and parallel computing. *Nature Methods* **9**:772.

De Freitas PD, Mendez FL, Chávez-Congrains K, Galetti PM, Coutinho LL, Pissinatti A, Bustamante CD. 2018. Next-generation sequencing of the complete mitochondrial genome of the endangered species black lion Tamarin *Leontopithecus chrysopygus* (Primates) and mitogenomic phylogeny focusing on the Callitrichidae family. *G3* **8**:1985–1991 DOI 10.1534/g3.118.200153.

DeLong ER, DeLong DM, Clarke-Pearson DL. 1988. Comparing the areas under two or more correlated receiver operating characteristic curves: a nonparametric approach. *Biometrics* **44**:837–845 DOI 10.2307/2531595.

Dierckxsens N, Mardulyn P, Smits G. 2017. NOVOPlasty: de novo assembly of organelle genomes from whole genome data. *Nucleic Acids Research* **45**:e18 DOI 10.1093/nar/gkw1060.

Dong Q, Shi L, Li Y, Jiang M, Sun H, Wang B, Cheng H, Zhang Y, Shao T, Shi Y, Wang Z. 2018. Differential responses of *Lasiopodomys mandarinus* and *Lasiopodomys brandtii* to chronic hypoxia: a cross-species brain transcriptome analysis. *BMC Genomics* **19**:901 DOI 10.1186/s12864-018-5318-1.

Dong Q, Wang Z, Jiang M, Sun H, Wang X, Li Y, Zhang Y, Cheng H, Chai Y, Shao T, Shi L. 2020. Transcriptome analysis of the response provided by *Lasiopodomys mandarinus* to severe hypoxia includes enhancing DNA repair and damage prevention. *Frontiers in Zoology* **17**:Article 9 DOI 10.1186/s12983-020-00356-y.

Drummond AJ, Ho SYW, Phillips MJ, Rambaut A. 2006. Relaxed phylogenetics and dating with confidence. *PLOS Biology* **4**:e88 DOI 10.1371/journal.pbio.0040088.

Drummond AJ, Rambaut A. 2007. BEAST: Bayesian evolutionary analysis by sampling trees. *BMC Evolutionary Biology* **7**:214 DOI 10.1186/1471-2148-7-214.

Elith J, Phillips SJ, Hastie T, Dudík M, Chee YE, Yates CJ. 2011. A statistical explanation of MaxEnt for ecologists. *Diversity and Distributions* **17**:43–57 DOI 10.1111/j.1472-4642.2010.00725.x.

Fawcett T. 2006. An introduction to ROC analysis. *Pattern Recognition Letters* **27**:861–874 DOI 10.1016/j.patrec.2005.10.010.

Finn RD, Clements J, Edd Eddy, SR. 2011. HMMER web server: interactive sequence similarity searching. *Nucleic Acids Research* **39**:W29–W37 DOI 10.1093/nar/gkr367.

Galtier N, Nabholz B, Glémin S, Hurst GDD. 2009. Mitochondrial DNA as a marker of molecular diversity: a reappraisal. *Molecular Ecology* **18**:4541–4550 DOI 10.1111/j.1365-294X.2009.04380.x.

Gao J, Yue LL, Jiang X, Ni L, Ashraf MA, Zhou Y, Li K, Xiao J. 2017. Phylogeographic patterns of *Microtus fortis* (Arvicolinae: Rodentia) in China based on mitochondrial DNA sequences. *Pakistan Journal of Zoology* **49**:1185–1195 DOI 10.17582/journal.pjz/2017.49.4.1185.1195.

Gernhard T. 2008. The conditioned reconstructed process. *Journal of Theoretical Biology* **253**:769–778 DOI 10.1016/j.jtbi.2008.04.005.

Gladkikh OL, Romanenko SA, Lemskaya NA, Serdyukova NA, O'Brien PC, Kovalskaya JM, Smorkatcheva AV, Golenishchev FN, Perelman PL, Trifonov VA, Graphodatsky AS. 2016. Rapid karyotype evolution in Lasiopodomys involved at least two autosome –sex chromosome translocations. *PLOS ONE* **11**:e0167653 DOI 10.1371/journal.pone.0167653.

Grant JR, Stothard P. 2008. The CGView Server: a comparative genomics tool for circular genomes. *Nucleic Acids Research* **36**:W181–W184 DOI 10.1093/nar/gkn179.

Gromov IM, Polyakov IY. 1978. *Fauna of the USSSR, mammals In: Voles (Microtinae)*. New Delhi: Smithsonian Inst. Libraries and the National Science Foundation.

Guo ZT, Sun B, Zhang ZS, Peng SZ, Xiao GQ, Ge JY, Hao QZ, Qiao YS, Liang MY, Liu JF, Yin QZ, Wei JJ. 2008. A major reorganization of Asian climate by the Early Miocene. *Climate of the Past* **4**:153–174 DOI 10.5194/cp-4-153-2008.

Heath TA, Huelsenbeck JP, Stadler T. 2014. The fossilized birth–death process for coherent calibration of divergence-time estimates. *Proceedings of the National Academy of Sciences of the United States of America* **111**:E2957–E2966.

Hijmans RJ, Cameron SE, Parra JL, Jones PG, Jarvis A. 2005. Very high resolution interpolated climate surfaces for global land areas. *International Journal of Climatology* **25**:1965–1978 DOI 10.1002/joc.1276.

Huang P, Carpenter JM, Chen B, Li TJ. 2019. The first divergence time estimation of the subfamily *Stenogastrinae* (Hymenoptera: Vespidae) based on mitochondrial phylogenomics. *International Journal of Biological Macromolecules* **137**:767–773 DOI 10.1016/j.ijbiomac.2019.06.239.

Humphreys AM, Rydin C, Jønsson KA, Alsop D, Callender-Crowe LM, Barraclough TG. 2016. Detecting evolutionarily significant units above the species level using the generalised mixed Yule coalescent method. *Methods in Ecology and Evolution* **7**:1366–1375 DOI 10.1111/2041-210X.12603.

Jain IH, Zazzeron L, Goli R, Alexa K, Schatzman-Bone S, Dhillon H, Goldberger O, Peng J, Shalem O, Sanjana NE, Zhang F, Mootha VK. 2016. Hypoxia as a therapy for mitochondrial disease. *Science* **352**:54–61 DOI 10.1126/science.aad9642.

Jiang M, Shi L, Li X, Dong Q, Sun H, Du Y, Zhang YF, Shao T, Cheng H, Chen WH, Wang Z. Genome-wide adaptive evolution to underground stresses in subterranean mammals: Hypoxia adaption, immunity promotion, and sensory specialization. *Ecology and Evolution* **10**:7377–7388 DOI 10.1002/ece3.6462.

Katoh K, Standley DM. 2013. MAFFT multiple sequence alignment software version 7: improvements in performance and usability. *Molecular Biology and Evolution* **30**:772–780 DOI 10.1093/molbev/mst010.

Kenechukwu NA, Li M, An L, Cui M, Wang C, Wang A, Chen Y, Du S, Feng C, Zhong S, Gao Y, Qi D. 2018. Comparative analysis of the complete mitochondrial genomes for development application. *Frontiers in Genetics* **9**:651.

Kohli BA, Speer KA, Kilpatrick CW, Batsaikhan N, Damdinbazar D, Cook JA. 2014. Multilocus systematics and non-punctuated evolution of *Holarctic myodini* (Rodentia: Arvicolinae). *Molecular Phylogenetics and Evolution* **76**:18–29 DOI 10.1016/j.ympev.2014.02.019.

Lehwark P, Greiner S. 2019. GB2sequin - a file converter preparing custom GenBank files for database submission. *Genomics* **111**:759–761 DOI 10.1016/j.ygeno.2018.05.003.

Li JQ, Li L, Fu BQ, Yan HB, Jia WZ. 2019. Complete mitochondrial genomes confirm the generic placement of the plateau vole, *Neodon fuscus*. *Bioscience Reports* **39(8)**:BSR20182349 DOI 10.1042/BSR20182349.

Li K, Kohn MH, Zhang S, Wan X, Shi DZ, Wang D. 2017. The colonization and divergence patterns of Brandt's vole (*Lasiopodomys brandtii*) populations reveal evidence of genetic surfing. *BMC Evolutionary Biology* **17**:145 DOI 10.1186/s12862-017-0995-y.

Li YK, Lu JQ, Wang ZL. 2016a. Complete mitochondrial genome of *Lasiopodomys mandarinus mandarinus* (Arvicolinae, Rodentia). *Mitochondrial DNA. Part A, DNA Mapping, Sequencing, and Analysis* **27**:1459–1460.

Li Y, Shi Y, Lu JQ, Ji W, Wang ZL. 2016b. Sequence and phylogenetic analysis of the complete mitochondrial genome of *Lasiopodomys mandarinus mandarinus* (Arvicolinae, Rodentia). *Gene* **593**:302–307 DOI 10.1016/j.gene.2016.08.035.

Liu M, Shi HX, Gao S, Song MJ. 2013. The introduction of Brandt's vole and its changes in names and systematic classification. *Chinese Journal of Comparative Medicine* **23**:53–57.

Liu S, Jin W, Liu Y, Murphy RW, Lv B, Hao H, Liao R, Sun Z, Tang M, Chen W, Fu J. 2017. Taxonomic position of Chinese voles of the tribe Arvicolini and the description of 2 new species from Xizang, China. *Journal of Mammalogy* **98**:166–182.

Liu S, Liu Y, Guo P, Sun Z, Murphy RW, Fan Z, Fu J, Zhang Y. 2012a. Phylogeny of oriental voles (Rodentia: Muridae: Arvicolinae): molecular and morphological evidence (Rodentia: Muridae: Arvicolinae). *Zoological Science* **29**:610–622 DOI 10.2108/zsj.29.610.

Liu SY, Sun ZY, Liu Y, Wang H, Guo P, Murphy RW. 2012b. A new vole from Xizang, China and the molecular phylogeny of the genus *Neodon* (Cricetidae: Arvicolinae). *Zootaxa* **3235**:1–22.

Lohse M, Drechsel O, Kahlau S, Bock R. 2013. OrganellarGenomeDRAW—a suite of tools for generating physical maps of plastid and mitochondrial genomes and visualizing expression data sets. *Nucleic Acids Research* **41**:W575–W581 DOI 10.1093/nar/gkt289.

Lowe TM, Eddy SR. 1997. TRNAscan-SE: a program for improved detection of transfer RNA genes in genomic sequence. *Nucleic Acids Research* **25**:955–964 DOI 10.1093/nar/25.5.955.

Malik A, Domankevich V, Lijuan H, Xiaodong F, Korol A, Avivi A, Shams I. 2016. Genome maintenance and bioenergetics of the long-lived hypoxia-tolerant and cancer-resistant blind mole rat, *Spalax*: a cross-species analysis of brain transcriptome. *Scientific Reports* **6**:38624 DOI 10.1038/srep38624.

Malik A, Korol A, Weber M, Hankeln T, Avivi A, Band M. 2012. Transcriptome analysis of the Spalax hypoxia survival response includes suppression of apoptosis and tight control of angiogenesis. *BMC Genomics* **13**:615 DOI 10.1186/1471-2164-13-615.

Martin A. 1995. Metabolic rate and directional nucleotide substitution in animal mitochondrial DNA. *Molecular Biology and Evolution* **12**:1124–1131.

Martin Y, Gerlach G, Schlötterer C, Meyer A. 2000. Molecular phylogeny of European muroid rodents based on complete cytochrome b sequences. *Molecular Phylogenetics and Evolution* **16**:37–47 DOI 10.1006/mpev.1999.0760.

Martínková N, Moravec J. 2012. Multilocus phylogeny of arvicoline voles (Arvicolini, Rodentia) shows small tree terrace size. *Folia Zoologica* **61**:254–267 DOI 10.25225/fozo.v61.i3.a10.2012.

Mezhzherin SV, Zykov AE, Morozov-Leonov SY. 1993. Biochemical variation and genetic divergence of palearctic voles (Arvicolidae), Meadow voles Microtus Schrank, 1798, snow voles, Chionomys Miller, 1908, water voles, Arvicola Lacepede, 1799. *Genetica* **29**:28–41.

Mueller RL. 2006. Evolutionary rates, divergence dates, and the performance of mitochondrial genes in Bayesian phylogenetic analysis. *Systematic Biology* **55**:289–300 DOI 10.1080/10635150500541672.

Nevo E. 2013. Stress, adaptation, and speciation in the evolution of the blind mole rat, Spalax, in Israel. *Molecular Phylogenetics and Evolution* **66**:515–525 DOI 10.1016/j.ympev.2012.09.008.

Nguyen LT, Schmidt HA, Haeseler Avon, Minh BQ. 2015. IQ-TREE: a fast and effective stochastic algorithm for estimating maximum-likelihood phylogenies. *Molecular Biology and Evolution* **32**:268–274 DOI 10.1093/molbev/msu300.

Ojala D, Montoya J, Attardi G. 1981. TRNA punctuation model of RNA processing in human mitochondria. *Nature* **290**:470–474 DOI 10.1038/290470a0.

Pamenter ME, Hall JE, Tanabe Y, Simonson TS. 2020. Cross-species insights into genomic adaptations to hypoxia. *Frontiers in Henetics* **11**:Article 743 DOI 10.3389/fgene.2020.00743.

Parsons PA. 2005. Environments and evolution: interactions between stress, resource inadequacy and energetic efficiency. *Biological Reviews* **80(4)**:589–610 DOI 10.1017/S1464793105006822.

Petrova TV, Tesakov AS, Kowalskaya YM, Abramson NI. 2016. Cryptic speciation in the narrow-headed vole *Lasiopodomys* (*Stenocranius*) *gregalis* (Rodentia: Cricetidae). *Zoologica Scripta* **45**:618–629 DOI 10.1111/zsc.12176.

Petrova TV, Zakharov ES, Samiya R, Abramson NI. 2015. Phylogeography of the narrow-headed vole *Lasiopodomys* (*Stenocranius*) *gregalis* (Cricetidae, Rodentia) inferred from mitochondrial cytochrome b sequences: an echo of Pleistocene prosperity. *Journal of Zoological Systematics and Evolutionary Research* **53**:97–108 DOI 10.1111/jzs.12082.

Pfeiffer F, Gröber C, Blank M, Händler K, Beyer M, Schultze JL, Mayer G. 2018. Systematic evaluation of error rates and causes in short samples in next-generation sequencing. *Scientific Reports* **8**:10950 DOI 10.1038/s41598-018-29325-6.

Phillips SJ, Anderson RP, Schapire RE. 2006. Maximum entropy modeling of species geographic distributions. *Ecological Modelling* **190**:231–259 DOI 10.1016/j.ecolmodel.2005.03.026.

Prost S, Guralnick RP, Waltari E, Fedorov VB, Kuzmina E, Smirnov N, Kolfschoten VT, Hofreiter K, Vrieling K. 2013. Losing ground: past history and future fate of A rctic small mammals in a changing climate. *Global Change Biology* **19(6)**:1854–1864 DOI 10.1111/gcb.12157.

Rambaut A, Drummond AJ, Xie D, Baele G, Suchard MA. 2018. Posterior summarization in Bayesian phylogenetics using Tracer 1.7. *Systematic Biology* **67**:901–904 DOI 10.1093/sysbio/syy032.

Ramos B, González-Acuña D, Loyola DE, Johnson WE, Parker PG, Massaro M, Dantas GP, Miranda MD, Vianna JA. 2018. Landscape genomics: natural selection drives the evolution of mitogenome in penguins. *BMC Genomics* **19**:53 DOI 10.1186/s12864-017-4424-9.

R Development Core Team. 2013. R: a language and environment for statistical computing. Vienna: R Foundation for Statistical Computing.

Rozas J, Ferrer-Mata A, Sánchez-DelBarrio JC, Guirao-Rico S, Librado P, Ramos-Onsins SE, Sánchez-Gracia A. 2017. DnaSP 6: DNA sequence polymorphism analysis of large data sets. *Molecular Biology and Evolution* **34**:3299–3302 DOI 10.1093/molbev/msx248.

Santore MT, McClintock DS, Lee VY, Budinger GRS, Chandel NS. 2002. Anoxia-induced apoptosis occurs through a mitochondria-dependent pathway in lung epithelial cells. *American Journal of Physiology. Lung Cellular and Molecular Physiology* **282**:L727–L734 DOI 10.1152/ajplung.00281.2001.

Shields CA, Bailey DA, Danabasoglu G, Jochum M, Kiehl JT, Levis S, Park S. 2012. The low-resolution CCSM4. *Journal of Climate* **25**:3993–4014 DOI 10.1175/JCLI-D-11-00260.1.

Solaini G, Baracca A, Lenaz G, Sgarbi G. 2010. Hypoxia and mitochondrial oxidative metabolism. *Biochimica et Biophysica Acta* **1797**:1171–1177 DOI 10.1016/j.bbabio.2010.02.011.

Stolper DA, Bender ML, Dreyfus GB, Yan Y, Higgins JA. 2016. A Pleistocene ice core record of atmospheric O_2 concentrations. *Science* **353**:1427–1430 DOI 10.1126/science.aaf5445.

Sun H, Zhang Y, Shi Y, Li Y, Li W, Wang Z. 2018. Evolution of the CLOCK and BMAL1 genes in a subterranean rodent species (*Lasiopodomys mandarinus*). *International Journal of Biological Macromolecules* **109**:932–940 DOI 10.1016/j.ijbiomac.2017.11.076.

Tian XY, Gu SM, Pan D, Shi LY, Wang ZL. 2020. The complete mitochondrial genome of *Lasiopodomys brandtii*. *Mitochondrial DNA Part B* **5**:364–365 DOI 10.1080/23802359.2019.1703567.

Tillich M, Lehwark P, Pellizzer T, Ulbricht-Jones ES, Fischer A, Bock R, Greiner S. 2017. GeSeq –versatile and accurate annotation of organelle genomes. *Nucleic Acids Research* **45**:W6–W11 DOI 10.1093/nar/gkx391.

Vasconcellos MM, Colli GR, Weber JN, Ortiz EM, Rodrigues MT, Cannatella DC. 2019. Isolation by instability: historical climate change shapes population structure and genomic divergence of treefrogs in the Neotropical Cerrado savanna. *Molecular Ecology* **28**:1748–1764 DOI 10.1111/mec.15045.

Wang C, Zhao X, Liu Z, Lippert PC, Graham SA, Coe RS, Yi H, Zhu L, Liu S, Li Y. 2008. Constraints on the early uplift history of the Tibetan Plateau. *Proceedings of the National Academy of Sciences of the United States of America* **105**:4987–4992 DOI 10.1073/pnas.0703595105.

Wang YX. 2003. *A complete checklist of mammal species and subspecies in China: a taxonomic and geographic reference*. Beijing: China Forestry Publishing House.

Watanabe S, Hajima T, Sudo K, Nagashima T, Takemura T, Okajima H, Nozawa T, Kawase H, Abe M, Yokohata T, Ise T, Kawamiya M. 2011. Miroc-ESM 2010: model description and basic results of CMIP5-20c3m experiments. *Geoscientific Model Development* **4**:845–872 DOI 10.5194/gmd-4-845-2011.

Wilson DE, Reeder DM. 2005. *Mammal species of the world: a taxonomic and geographic reference*. 3rd edition. Baltimore: Johns Hopkins University Press.

Witt KE, Huerta-Sánchez E. 2019. Convergent evolution in human and domesticate adaptation to high-altitude environments. *Philosophical Transactions of the Royal Society of London Series B, Biological Sciences* **374**:20180235 DOI 10.1098/rstb.2018.0235.

Xie W, Lewis PO, Fan Y, Kuo L, Chen MH. 2011. Improving marginal likelihood estimation for Bayesian phylogenetic model selection. *Systematic Biology* **60**:150–160 DOI 10.1093/sysbio/syq085.

Yang Z. 2007. PAML 4: phylogenetic analysis by maximum likelihood. *Molecular Biology and Evolution* **24**:1586–1591 DOI 10.1093/molbev/msm088.

Zhang Z, Cheng QQ, Ge Y. 2019. The complete mitochondrial genome of *Rhynchocypris oxycephalus* (Teleostei: Cyprinidae) and its phylogenetic implications. *Ecology and Evolution* **9**:7819–7837 DOI 10.1002/ece3.5369.

Zhang JY, Zhang LP, Yu DN, Storey KB, Zheng RQ. 2018. Complete mitochondrial genomes of *Nanorana taihangnica* and *N. yunnanensis* (Anura: Dicroglossidae) with novel gene arrangements and phylogenetic relationship of Dicroglossidae. *BMC Evolutionary Biology* **18**:26 DOI 10.1186/s12862-018-1140-2.

Zorenko T, Atanasov N. 2017. Patterns of behaviour as an evidence for the taxonomical status of *Lasiopodomys* (*Stenocranius*) *gregalis* (Pallas, 1779) (Rodentia: Arvicolinae). *Acta Zoologica Bulgarica. Supplement* **8**:189–197.